Spatial Resolution of Visual Stimuli in SSVEP-based Brain-Computer Interface

Jing Mu, David B. Grayden, Ying Tan, and Denny Oetomo

***Abstract*— Communicating spatial coordinates plays a crucial role in human-robot interactions, where a given target, object, or location needs to be localized. The steady-state visual evoked potential (SSVEP) is one of the most robustly detectable signals in electroencephalography (EEG)-based brain-computer interfaces (BCIs). However, the spatial resolution of the visual stimuli in a SSVEP-based BCI needs to be characterized for localization applications. In this study, we demonstrate that the influence of an adjacent stimulus attenuates to the baseline level when it is outside the paracentral region of human field of view (FOV) based on data collected from five subjects. This conservatively defines the spatial resolution in SSVEP. A potential lateral inhibition phenomenon was also observed when the two stimuli were immediately next to each other, which may reflect the center-surround structure of the receptive fields in visual cortex. Moreover, different frequency setups appear to affect the robustness of the SSVEP-based BCI and suggest that adjacent stimuli should be with frequencies that are more distinguishable visually.**

I. INTRODUCTION

Detecting intended spatial coordinates from a human user plays an important role in the capability to interact with machines, robots, and advanced prostheses, where a given target, object, or location needs to be localized. Brain-computer interfaces (BCIs) based on electroencephalography (EEG) are widely used as a tool to detect human intention. Steady-state visual evoked potentials (SSVEP) are robust signals in BCIs [1]. The major advantages of SSVEP are the relatively high information transfer rate (ITR), high signal-to-noise ratio (SNR), and minimal human training required [2], [3]. Currently, SSVEPs are widely used in BCI spellers and in triggering basic robotic commands.

To communicate an intended spatial location (spatial coordinates) through a BCI, it is necessary to characterize the spatial resolution that can be obtained between multiple SSVEP stimuli. In other words, it is important to know the proximity of two SSVEP stimuli, in the form of flashing lights of two distinct frequencies, that allows them to be distinguished or the amount of interference that one stimulus causes on another when both are in the field of view (FOV) of a subject.

Spatial resolution in the SSVEP visual stimuli has been a challenging problem and existing studies have circumvented this by placing the stimuli spatially distant from each other. The SSVEP-based BCI telephone keypad [4], with 12 blocks of stimuli on the screen, was developed with the spacing between the blocks designed to be much wider than the size of the blocks. The integrated version of the Bremen BCI speller, introduced in 2008 [5], navigated a cursor by five flashing blocks that were spread out to the corners and edges of the screen. Four light emitting diodes (LEDs) utilized for the control of a hand prosthesis [6] were spaced as far from each other as practical for the control of pronation, supination, and hand open/close. One LED was placed on the index finger, one on the little finger, and two on the forearm $7.5cm$ apart. A brain-controlled wheelchair was developed [7] with four flashing strips indicating predefined destination positions and orientations. The four strips were spaced out onto the four edges of the screen. Two LEDs were placed on a hand orthosis for the subject for command of the orthosis [8], in which the two LEDs were placed at least $9cm$ apart. A three-class SSVEP-based BCI for a meal assistance robot [9] determined target food holder position using three LED matrices that were placed next to the corresponding food holders and were clearly separated from each other.

Different approaches have been investigated to improve the accuracy of SSVEP detection [10], [11] and to improve the efficiency of visual stimulation [12], [13], [14], [15], [16]. As a rule-of-thumb, stimuli should be sufficiently separated spatially and should use as few visual stimulation units as possible. However, this strongly limits the number of stimulation units that can be used within a given area or workspace in the interface design, such as a computer screen or a table. Therefore, it is crucial to understand the limitations of spatial resolution in SSVEP-based BCIs to be able to extend the application of SSVEP-based BCIs to more complex tasks, such as serving as a target localization tool in a robotic arm reaching task.

In this research, we investigated the effect of the distance between two visual stimuli on the frequency responses of brain signals measured using EEG. Experiments were carried out with the visual stimuli placed at different distances from each other in horizontal and vertical directions. The results and conclusions from this paper can be used as a guideline for stimuli setup in SSVEP-based BCIs. Similar experimental protocol can be used to calibrate SSVEP-based BCIs when a large number of options needs to be presented to users.

II. METHODS

The aim of the study was to characterize the spatial resolution of SSVEP stimuli. An SSVEP stimulus was realized in the form of a 3×3 block of LEDs, flashed at a given frequency. The attenuation of the SSVEP signal obtained

J Mu, Y Tan and D Oetomo are with School of Electrical, Mechanical and Infrastructure Engineering, DB Grayden is with the Department of Biomedical Engineering, The University of Melbourne, Parkville, VIC 3010, Australia. j.mu@student.unimelb.edu.au, {grayden, yingt, doetomo}@unimelb.edu.au

through EEG was recorded as one stimulus block was shifted with increasing distances along the plane normal to the subject's visual line (see Figure 1a). This was done while the subject maintained their gaze at the stationary stimulus at the center of the plane.

A. Hardware Setup

The overall hardware setup of the experiment is shown in Figure 1. Subjects were asked to sit in front of a LED board that had 832 RGB LEDs formed into a plus (+) shape. The pattern measured $50cm$ horizontally and vertically, made up of 56 LEDs in length and 8 LEDs wide. Each RGB LED was $5mm \times 5mm$ in size and the gap between adjacent LEDs was $4mm$. The distance between the LED board and the subject was maintained at $80cm$ with eye height at the middle of the board (Figure 1b). The top left LED among the four LEDs in the center of the board was assigned as the "Center Point" (CP) and it was on the sagittal plane of the subject.

Electroencephalograms were recorded using a g.USBamp EEG system with g.SAHARA dry electrodes (g.tec medical engineering, Austria) and sampled at $512Hz$. A $50Hz$ notch filter was applied when collecting data (g.tec provided standard filter to remove the noise from the standard power supply frequency). In this experiment, 8 electrodes were placed according to the standard international 10-20 system. The selected EEG electrode locations were: Oz, O1, O2, POz, PO3, PO4, C1, and C2. All experiments were conducted in a Faraday shielded room in the Centre for Neural Engineering, The University of Melbourne.

B. Subjects

Five healthy subjects (two females and three males, aged 24-35 years) participated in the experiment. Subjects 2 and 4 wore glasses. No subjects had previous experience with EEG or brain-computer interfaces. This experiment was approved by the University of Melbourne Human Research Ethics Committee (Ethics ID: 1851283).

C. Experimental Protocol

In the experiment, two 3×3 LED blocks were flashed at different frequencies in red color ($\lambda = 620 - 630nm$). One LED block was centered at the CP and is referred to as the "Fixed Block" (FB). The other LED block was presented at different locations along an axis, shifting further away from the FB as experiment progressed; we call this the "Shifting Block" (SB) (see Figure 1a). The experiment consisted of three sessions; in each session, all four directions (Up, Down, Left, and Right) were examined in four sub-sessions. There were 24 location steps presented in each direction, which are heretofore referred to as Step 1, Step 2, ..., Step 24.

The FB frequency was kept at $8Hz$ for all sessions. The SB frequency was set to $10Hz$, $20Hz$, and $30Hz$, in the three sessions, respectively. A one-minute break and a five-minute break were placed between the sub-sessions and sessions, respectively. The subjects were asked to keep silent and sit still during the trials. The subjects were asked to fixate on the FB during the experiments and the SB was shifted

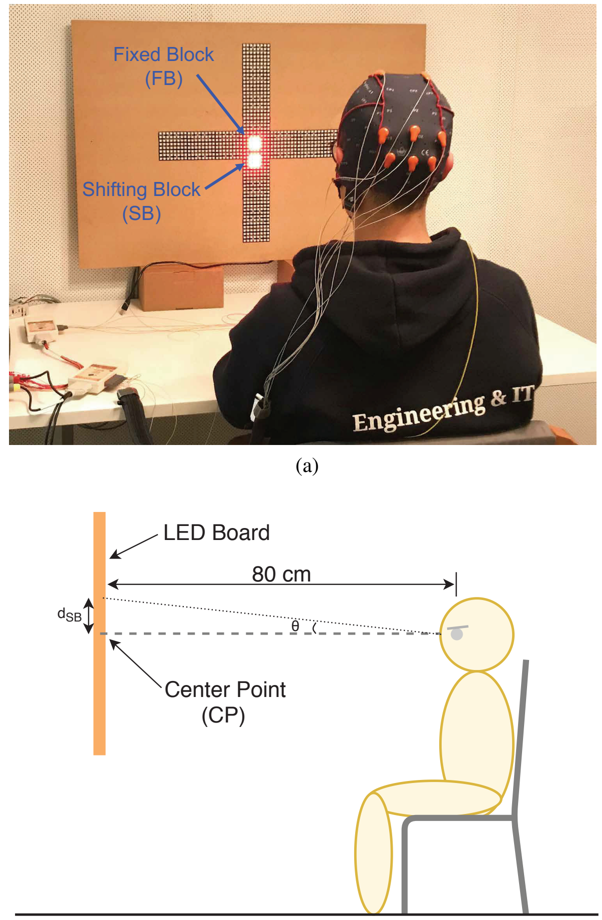

(a)

(b)

Fig. 1: Hardware setup. (a) The fixed block (FB) is at the center of the LED board and the shifting block (SB) moves away from the FB as experiment proceeds. (b) The subject sits in front of the LED board with their eyes horizontally aligned with the focus point and the board placed approximately $80cm$ from the subject. θ and d_{SB} can be calculated using Equations (1) and (2), respectively.

one row or column away from the FB every five seconds starting from the block immediately adjacent to the FB in the testing direction. The FB was turned on (not flashing) for ten seconds at the beginning of each trial to help subjects focus on the FB.

D. Data Analysis

As mentioned above, 8 electrodes were placed for the EEG measurements. However, as some subjects produced frequent limb motions during the trials, the measurements from C1 and C2 were discarded. Noise cancellation will be explained in Section III.

The data collected over the occipital lobe (Oz, O1, O2, POz, PO3 and PO4) were averaged and then a band-pass filter with frequencies $5-45Hz$ was applied to the data using the MATLAB function "bandpass" with 'ImpulseResponse' set to 'auto', 0.85 'Steepness', and $60dB$ 'StopbandAttenuation'. Fast Fourier transforms (FFTs) were performed on the filtered data with a window of five seconds and 2560 samples of data (in accordance to the time of each Step described in Section II-C and the sampling rate), and the magnitudes at $8Hz$ (FB frequency) and the SB frequency (10, 20, or $30Hz$) were extracted. The FFT magnitudes at each step were averaged over the four directions (Up, Down, Left, Right) within each session. Finally, these averaged FFT magnitudes were plotted against step index, which is also converted to the vision angle for the presentation of results.

III. Results

In this section, results are presented and the procedure to produce the results is explained. The intermediate results from the $20Hz$ SB frequency session are shown as an example.

Figure 2 shows the averaged FFT magnitudes across four directions for each subject and plotted against step index and vision angle. From the top figure in Figure 2, it can be seen that the $8Hz$ FFT magnitudes for each subject are roughly constant with some fluctuations. In Steps 15-24 on the bottom figure in Figure 2, the FFT magnitudes are also nearly constant for each subject. By running the Jarque-Bera test with MATLAB command jbtest, we confirmed that the $8Hz$ data and $20Hz$ data between Steps 15-24 were normally distributed at a 5% significance level for each subject. The $8Hz$ values were likely to be constant because this is where the subjects fixated. The $20Hz$ values beyond Step 15 likely represented normal background EEG signals. Therefore, the following steps were taken to produce the normalized results as shown in Figure 3.

(i) Calculate the nominal magnitude at $8Hz$ by averaging over all steps for each subject.
(ii) Calculate the baseline magnitude at $20Hz$ by taking the average of Steps 15-24 for each subject.
(iii) Calculate the unbiased $20Hz$ data by subtracting the baseline magnitude from the data.
(iv) Calculate the unbiased $8Hz$ magnitudes by subtracting the baseline magnitude from the $8Hz$ nominal magnitude.
(v) Calculate the ratio by dividing the unbiased $20Hz$ data by the unbiased $8Hz$ magnitudes.

A. Results from $20Hz$ SB Frequency

The results in Figure 3a show a consistent decreasing trend from Step 2 onward, and settle to the baseline level after Step 5. The step distances can be standardized by calculating the vision angle between the center of FB and the edge of SB that is closest to FB using:

$$\theta = arctan\left(\frac{d_{SB}}{d_{sub}}\right), \tag{1}$$

$$d_{SB} = \left(\frac{w_{FB}}{2} + S - \frac{1}{2}\right) d_{LED} - \frac{1}{2} w_{LED}, \tag{2}$$

where θ is the vision angle, d_{SB} is the distance between the center of FB and the close edge of SB, d_{sub} is the distance between the subject and the LED board, w_{FB} is the dimension of the FB, S is the step index ($S = 1, ..., 24$), d_{LED} is the distance between the centers of two adjacent LEDs, and w_{LED} is the width of each LED.

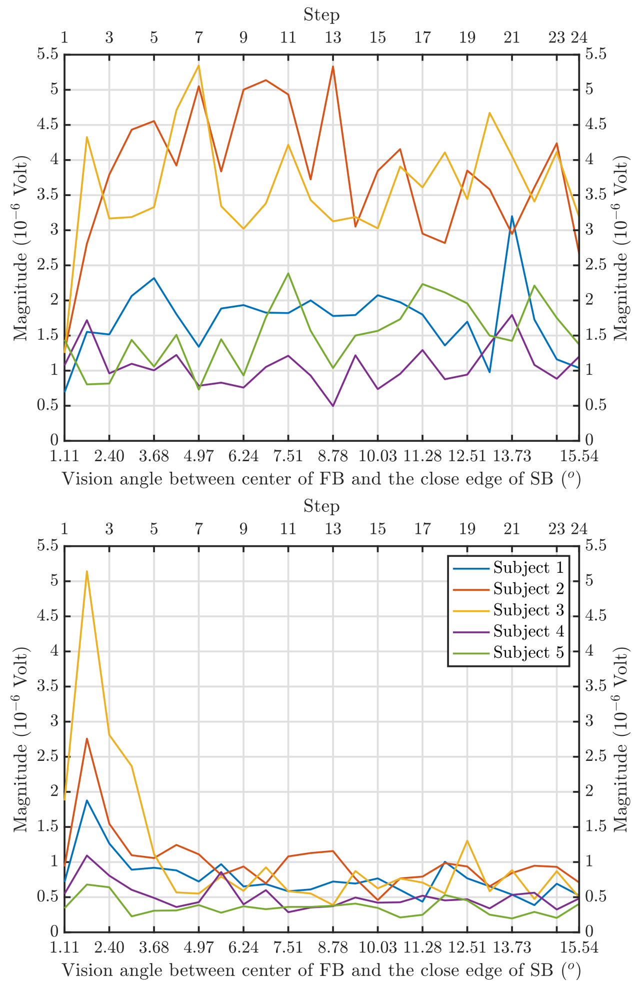

Fig. 2: Average FFT magnitudes across four directions vs. step index and vision angle within the $20Hz$ session. Top: The average of the FFT values at each step at $8Hz$ from the four directions for the five subjects, where each subject's result is indicated with a different line color. Bottom: The average of the FFT value at $20Hz$ from the four directions for the five subjects.

Substituting $d_{sub} = 800\ mm$, $w_{FB} = 3$, $d_{LED} = 9\ mm$, $S = 5$, and $w_{LED} = 5\ mm$ into the equations, we get $\theta \approx 3.68°$, which falls within but close to the boundary of the central and paracentral region (an $8°$ opening angle cone) of human field of view (FOV) [17]. Thus, the region of greatest attenuation of $20Hz$ is outside the central and paracentral region of the human FOV.

B. Results from 10 and $30Hz$ SB Frequencies

Experiments were also conducted with $10Hz$ and $30Hz$ SB frequencies. As shown in Figure 3b, the $30Hz$ SB frequency session produced a similar result to that observed in the $20Hz$ SB frequency session. Results from $10Hz$ session is not shown here because the signals collected contain too much noise and hardly provide any meaningful

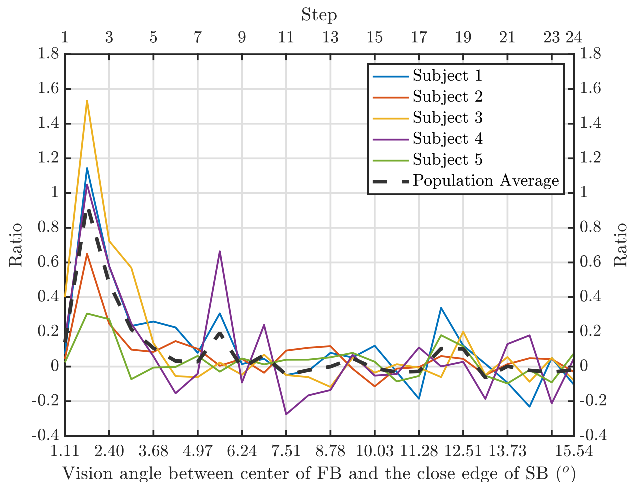

(a) Ratio between magnitudes at $8Hz$ and $20Hz$ with baseline bias removed

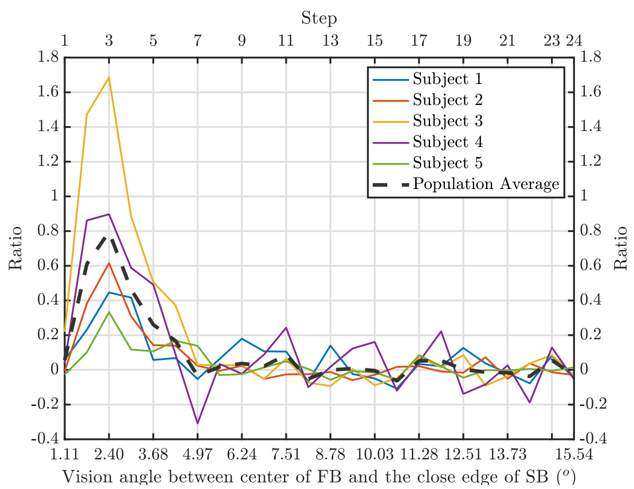

(b) Ratio between magnitudes at $8Hz$ and $30Hz$ with baseline bias removed

Fig. 3: The normalized results for SB at 20, and $30Hz$. The plots show the ratio between the magnitude of the unbiased data at SB frequency and the nominal magnitude at $8Hz$ (FB frequency). (a) SB at $20Hz$. (b) SB at $30Hz$.

information. This may be attributed to the fact that the SB frequency of $10Hz$ being very close to that of the FB ($8Hz$). This will be further investigated in the future.

IV. Discussion

The results from this experiment provide three key findings: the attenuation in magnitude at the Shifting Block (SB) frequency as lateral distance increased; the existence of the significant suppression at Step 1 on both Fixed Block (FB) and SB frequencies; and variations in responses when SB was set to different frequencies.

In this paper, the spatial resolution is defined as the vision angle cone within which no other stimulus should be found. Note that in this experiment, the stimuli are not of zero width, hence introduce a maximum of $\pm 0.82°$ uncertainty.

A. Magnitude Attenuation at SB Frequency with Distance

By reading the population average of our five subjects (plotted in black dashed line) in Figure 3, we can see that, on average, $2.40°$ vision angle (Step 3) gives an attenuation of 50% at the SB frequency in $20Hz$ session. A conservative spatial resolution (attenuates to baseline level) requires a $4.32°$ vision angle (Step 6) in the $20Hz$ session.

In the $30Hz$ session, the population average suggests that the 50% attenuation happens at around $3.04°$ (Step 4), and $4.97°$ (Step 7) guarantees the conservative spatial resolution.

In general, from the observations above, the central region (a $5°$ opening angle cone) of human FOV corresponds to an intermediate spatial resolution with 50% attenuation at SB frequency, and the paracentral region of human FOV guarantees a conservative spatial resolution (fully attenuated to baseline) within the uncertainty margin.

B. Suppression at Step 1

Another distinct feature observed from our results was consistent suppression at Step 1 for most subjects in both FB and SB frequencies[1]. This may be due to the center-surround structure of the receptive field in visual cortex [18]. The center-surround structure suggests that there exists an inhibitory region surrounding the excitatory region at a relatively small distance. As the FB and SB are immediately next to each other at Step 1, each is within the inhibitory surround region of the other. The suppression on both $8Hz$ and $20Hz$ plots supports this hypothesis.

This lateral inhibition suggests that the distance between two adjacent visual stimuli should be selected carefully. An inappropriate short distance might depress the robustness of SSVEP-based BCI.

C. Variation with SB Frequencies

As mentioned in Section III-B, the $10Hz$ result does not show similar features as the results from $20Hz$ and $30Hz$ sessions. A possible explanation of this inconsistent result could be that the frequencies $8Hz$ and $10Hz$ are too close to each other and are difficult to distinguish visually.

The results from the $20Hz$ and $30Hz$ sessions demonstrate consistent features in attenuation and suppression. However, the attenuation readings presented in Section IV-A and the shift in peak locations suggest that the spatial resolution could be dependent on the SB frequency.

These variations between different SB frequencies indicates that the frequencies on the two adjacent visual stimuli should be designed so that they are visually distinguishable, and calibration might be required on different frequency settings. Further investigation of the use of other frequencies is warranted.

[1] In Figure 2 (top figure), subject 5 has a larger magnitude at Step 1 than Step 2, however, the magnitude at Step 1 (1.4393×10^{-5} V) is still lower than the nominal magnitude (1.5122×10^{-5} V).

V. Conclusion

In this study, we examined the spatial resolution of visual stimuli in SSVEP-based BCI by gradually moving a flashing block (SB) away from another flashing block (FB) at the fixation point. In general, the intermediate and conservative spatial resolution coincides with the central and paracentral region of human FOV. Consistent suppression at Step 1 (stimuli immediate adjacent) was found in most subjects at both FB and SB frequencies, which we hypothesize is due to the center-surround structure of visual neurons. The variation of the result between different SB frequencies could serve as a guide on the selection of frequencies for BCIs.

Some of the reasons behind the observed patterns are still not sufficiently clear and require further studies. Extended experiments should be done within the magnitude suppression region to investigate the detailed response curve. The effect of changing different frequencies on adjacent stimuli can also be further studied.

References

[1] B. Allison, T. Luth, D. Valbuena, A. Teymourian, I. Volosyak, and A. Graser, "BCI demographics: How many (and what kinds of) people can use an SSVEP BCI?" *IEEE Transactions on Neural Systems and Rehabilitation engineering*, vol. 18, no. 2, pp. 107–116, 2010.

[2] G. Bin, X. Gao, Z. Yan, B. Hong, and S. Gao, "An online multi-channel SSVEP-based brain–computer interface using a canonical correlation analysis method," *Journal of Neural Engineering*, vol. 6, no. 4, p. 046002, 2009.

[3] L. F. Nicolas-Alonso and J. Gomez-Gil, "Brain computer interfaces, a review," *Sensors*, vol. 12, no. 2, pp. 1211–1279, 2012.

[4] M. Cheng, X. Gao, S. Gao, and D. Xu, "Design and implementation of a brain-computer interface with high transfer rates," *IEEE Transactions on Biomedical Engineering*, vol. 49, no. 10, pp. 1181–1186, 2002.

[5] D. Valbuena, I. Sugiarto, and A. Gräser, "Spelling with the Bremen brain-computer interface and the integrated SSVEP stimulator," in *Proceedings of the 4th International Brain-Computer Interface Workshop and Training Course*, 2008, pp. 291–296.

[6] G. R. Muller-Putz and G. Pfurtscheller, "Control of an electrical prosthesis with an SSVEP-based BCI," *IEEE Transactions on Biomedical Engineering*, vol. 55, no. 1, pp. 361–364, 2008.

[7] S. T. Müller, W. C. Celeste, T. F. Bastos-Filho, and M. Sarcinelli-Filho, "Brain-computer interface based on visual evoked potentials to command autonomous robotic wheelchair," *Journal of Medical and Biological Engineering*, vol. 30, no. 6, pp. 407–415, 2010.

[8] R. Ortner, B. Z. Allison, G. Korisek, H. Gaggl, and G. Pfurtscheller, "An SSVEP BCI to control a hand orthosis for persons with tetraplegia," *IEEE Transactions on Neural Systems and Rehabilitation Engineering*, vol. 19, no. 1, pp. 1–5, 2011.

[9] C. J. Perera, I. Naotunna, C. Sadaruwan, R. A. R. C. Gopura, and T. D. Lalitharatne, "SSVEP based BMI for a meal assistance robot," in *Systems, Man, and Cybernetics (SMC), 2016 IEEE International Conference on*. IEEE, 2016, pp. 002 295–002 300.

[10] Z. Wu and D. Yao, "Frequency detection with stability coefficient for steady-state visual evoked potential (SSVEP)-based BCIs," *Journal of Neural Engineering*, vol. 5, no. 1, pp. 36–43, 2007.

[11] E. Yin, Z. Zhou, J. Jiang, Y. Yu, and D. Hu, "A dynamically optimized SSVEP brain–computer interface (BCI) speller," *IEEE Transactions on Biomedical Engineering*, vol. 62, no. 6, pp. 1447–1456, 2015.

[12] T. S. Mukesh, V. Jaganathan, and M. R. Reddy, "A novel multiple frequency stimulation method for steady state VEP based brain computer interfaces," *Physiological Measurement*, vol. 27, no. 1, pp. 61–71, 2005.

[13] K.-K. Shyu, P.-L. Lee, Y.-J. Liu, and J.-J. Sie, "Dual-frequency steady-state visual evoked potential for brain computer interface," *Neuroscience Letters*, vol. 483, no. 1, pp. 28–31, 2010.

[14] C. Jia, X. Gao, B. Hong, and S. Gao, "Frequency and phase mixed coding in SSVEP-based brain–computer interface," *IEEE Transactions on Biomedical Engineering*, vol. 58, no. 1, pp. 200–206, 2011.

[15] Y. Zhang, P. Xu, T. Liu, J. Hu, R. Zhang, and D. Yao, "Multiple frequencies sequential coding for SSVEP-based brain-computer interface," *PloS One*, vol. 7, no. 3, p. e29519, 2012.

[16] H.-J. Hwang, D. H. Kim, C.-H. Han, and C.-H. Im, "A new dual-frequency stimulation method to increase the number of visual stimuli for multi-class SSVEP-based brain–computer interface (BCI)," *Brain Research*, vol. 1515, pp. 66–77, 2013.

[17] W. H. Swanson and G. E. Fish, "Color matches in diseased eyes with good acuity: detection of deficits in cone optical density and in chromatic discrimination," *JOSA A*, vol. 12, no. 10, pp. 2230–2236, 1995.

[18] D. Fitzpatrick, "Seeing beyond the receptive field in primary visual cortex," *Current Opinion in Neurobiology*, vol. 10, no. 4, pp. 438–443, 2000.